Applicability of three-parameter equation of state of solids: compatibility with first principles approaches and application to solids

2003 J. Phys.: Condens. Matter 15 1643

(http://iopscience.iop.org/0953-8984/15/10/313)

INSTITUTE OF PHYSICS PUBLISHING JOURNAL OF PHYSICS: CONDENSED MATTER

J. Phys.: Condens. Matter **15** (2003) 1643–1663 PII: S0953-8984(03)34935-5

Applicability of three-parameter equation of state of solids: compatibility with first principles approaches and application to solids

Papiya Bose Roy and Sushil Bose Roy

Department of Chemistry, TM Bhagalpur University, Bhagalpur 812001, India

Received 15 March 2002, in final form 8 January 2003
Published 3 March 2003
Online at stacks.iop.org/JPhysCM/15/1643

Abstract

In a recent paper we have proposed a three-parameter equation of state (EOS) of solids, and applied it to a few isotherms and shown that the fits are uniformly excellent. In this paper a comprehensive comparison of the applicability of our model is made with seven existing three-parameter EOSs. We have applied our model along with seven existing three-parameter EOSs, with no constraint on the parameters, to accurate and model-independent isotherms of nine solids and studied the fitting accuracy and agreement of the fit parameters with experiment. Further, each of these nine isotherms is divided into three subsets, and the resulting subsets fitted with all the eight EOSs. The stability of the fitted stress-free bulk modulus B_0 and its pressure derivatives B_0' and B_0'' with variation in the compression range is compared. Furthermore, our EOS is applied to a large number of inorganic as well as organic solids, including alloy, glasses, rubbers and plastics; of widely divergent bonding and structural characteristics, and a very good agreement is observed with the compression data. We have also studied the variation of bulk modulus with pressure, with reference to the data on NaCl and Ne, and noted a very good agreement. In addition, our model is applied, with B_0 and B_0' constrained to the theoretical values, to the five isotherms of MgO at 300, 500, 1000, 1500 and 2000 K, obtained on the basis of a first principles approach. For three of these isotherms, the fitting accuracy yielded by our model is higher than those by the three-parameter Birch and universal formulations. Further, variation of bulk modulus with pressure, and pressure with compression, is studied, and a good agreement is observed between the theoretical values and predictions. Furthermore, it is shown that our model agrees well with the theoretical isotherms of CsI and the fit parameters are in good agreement with the experimental data. In essence, the present study assesses the relative merits of the EOSs considered, in respect of applicability to the experimental isotherms with pressures ranging from low to a maximum that varies from the high to ultrahigh pressure regime; for the purposes of smoothing, interpolation and extraction of accurate values of bulk moduli. An overall inter-comparison of the calculated results for eight EOSs

decisively demonstrates the drastic superiority of our model on three counts: the fitting accuracy, stability of the fit parameters with variation in the compression range and agreement of the fit parameters with experiment.

1. Introduction

A constant search for an equation of state (EOS) of a condensed system, spanning over a century [1, 2], has culminated in the formulation of a number of EOSs [3–12], with varying degrees of success in describing the compressional behaviour of materials at high pressure. In a recent paper [12] we have proposed a new three-parameter EOS and applied it to a few isotherms to show that the fits are uniformly excellent, and equally excellent is the agreement of the fit parameters with experiment. The basic aim of the present paper is to ascertain the relative merit of our model with respect to applicability to the EOS data *vis-à-vis* the seven existing three-parameter EOSs, to show the compatibility of our model with first principles approaches, and its fitting capability features for a broad class of materials.

There are two distinct approaches to the study of pressure–volume relations of solids at high pressure. First, experimentally determined values of isothermal bulk modulus B_0 and its pressure derivative B_0' are used as inputs in an EOS and the resulting compression curve is compared with experiment. Second, an EOS is fitted to the experimental compression data and the fit bulk moduli parameters, calculated as coefficients, are compared with the independently measured experimental values, and further, the predicted isotherm based on the fit parameters is compared with experiment. However, objections are sometimes raised against the second approach to discriminate between EOSs [13, 14]. The reason advanced is that bulk modulus is a physical quantity, having a unique value at a specified thermodynamic state, while in the fitting procedures the bulk moduli are treated as coefficients, and as such cannot be used to discriminate between EOSs. But it can be seen that these objections are unrealistic from an experimental point of view. In the first approach it is assumed that the input experimental values are unique and real or at best lie within a narrow band of uncertainty. Now the moot point is whether there are any such measured values of the bulk modulus for any material. To illustrate the point, the measured values of bulk modulus for NaCl may be referred to. NaCl has a simple structure. There are over 20 sets of experimental values of bulk modulus available for NaCl [6, 15, 16]. Birch [6] presents a comparison of various data sets of measured bulk modulus values for NaCl. To the comparison list of Birch, some recent measurements are appended. A static measurement by Sorensen [17] gives $B_0 = 238$ kbar, $B_0' = 4.0$ and $B_0'' = 0.01$ kbar^{-1}. Recent ultrasonic values of Kim [18] are $B_0 = 235.6$ kbar, $B_0' = 5.11$ and $B_0'' = -0.000\,34$ kbar^{-1}, while the most recent model-independent infrared measurement by Hofmeister [16] suggests $B_0' = 4.59$ and $B_0'' = -0.0035$ kbar^{-1}.

Although, in principle, the ultrasonic method is intrinsically very precise (∼001%) [19], but it is not so impeccable in practice [6, 16]. Comparison of the various data sets for NaCl [6] suggests an uncertainty of over 2 and 10% in B_0 and B_0', respectively, derived from the ultrasonic studies. However, the problem of ascertaining the real values is not confined to this domain of uncertainty. If we turn to the value of $B_0' = 5.352$, from the highly regarded ultrasonic studies of Spetzler [20], it differs from the latest spectroscopic value of Hofmeister [16] by about 17%. It may be noted that Hofmeister claims that total errors in their measured value for NaCl could be as much as 1% only. A disagreement, of about 24%, from the value of Hofmeister [16] can be calculated on considering the value of $B_0' = 5.7$ from the highly regarded studies of Chhabildas [21], while a still larger disagreement, of over 40%, exists between the value of Chhabildas [21] and a recently measured value of Sorensen [17], as referred to above. Thus the

discrepancy, observed between the experimental values of B_0', is too large to be accounted for on the basis of experimental error or the use of various analytic techniques for data reduction. The implication of the attempt by Hofmeister [16] to explain away this anomaly: 'The various determinations of B_0' are equal within this larger uncertainty', is not clear because the serious question on the selection of data remains unanswered. The literature is replete with examples, where workers have chosen a particular set of bulk moduli that best suits enforcing the validity or utility of their models, and thus leading to ambiguity in data interpretation. The obvious conclusion to be reached is that the study of the compressional behaviour of materials by using experimental values of bulk modulus as inputs are overoptimistic and unrealistic exercises, until and unless the point of the high degree of ambiguity in the measured values of the bulk modulus is resolved.

McDonald [22] has suggested some important tests to discriminate between EOSs using a least-squares-fit technique. In line with [22], we have fitted our model to model-independent isotherms of nine solids and compared the fitting accuracy with seven existing three-parameter EOSs. It is observed that the fitting accuracy yielded by our model is substantially higher than those by the others. The fit values of B_0, resulting from all the EOSs, compare well with the data from the literature. However, the values of B_0' yielded by our model are remarkably close to experiment. Further, each of the nine isotherms is divided into three subsets with decreasing compression range. Also the EOSs are fitted to these subsets to assess the stability of B_0, B_0' and B_0'' with variation in the compression range. The stability, inferred from our model, is remarkably higher than from all the seven EOSs compared.

Aside from these tests, we have studied the variation of bulk modulus as a function of pressure for NaCl [20] and Ne [23] and noted a very good agreement with the experimental data. In addition, we have fitted our model to the isotherms of a large number of inorganic and organic solids, including alloy, glasses, plastics and rubbers; of widely divergent bonding and structural characteristics; and noted a very good agreement between the data and fits. Furthermore, we have shown that our model is compatible with the isotherms of CsI [24] and MgO [25, 26], derived on the basis of first principles approaches.

2. Empirical equations of state

In general, two-parameter EOSs prove inadequate for a successful description of the compression data of a broad class of solids, especially in the high pressure/compression ranges [27–29], as compared to their three-parameter counterparts. In this section the three-parameter EOSs we plan to inter-compare with are presented. Constancy of temperature is assumed throughout and no special notation is used.

The three-parameter Murnaghan EOS (abbreviated M3), which is based on a Taylor expansion of the isothermal bulk modulus to second order in terms of the pressure [30], is

$$V/V_0 = [(2 + (B_0' - \Gamma)(P/B_0))/(2 + (B_0' + \Gamma)(P/B_0))]^{1/\Gamma}, \tag{1}$$

with $\Gamma^2 = B_0'^2 - 2B_0B_0'' > 0$.

There are two improved versions of the M3 EOS available in the literature. The first one proposed by Luban (LU) [8], and extensively used by Anderson *et al* [8], can be presented as

$$V/V_0 = \exp\{(-1/\alpha^2 B_0)[\alpha\beta P + (\alpha - \beta)\ln(1 + \alpha P)]\}, \tag{2}$$

with $B_0' = B_0(\alpha - \beta)$ and $B_0'' = -2\beta B_0'$.

The second improved version was proposed by Kumari and Dass (KD) [11], which can be expressed explicitly in terms of B_0, B_0' and B_0'' as

$$V/V_0 = [(1 + m)\{\exp -(PB_0'')/B_0'\} - m]^{-(1/n)}, \tag{3}$$

with $m = \{-(B_0'^2)/(B_0B_0'')\}$ and $n = B_0' - (B_0B_0''/B_0')$.

Birch [5, 6] developed an expression based on the Eulerian strain measure $f = [(V_0/V)^{2/3} - 1]/2$. A Taylor expansion of the strain energy in terms of f, truncated at the fourth-order term of energy in strain, yields the following three-parameter EOS (B3):

$$P = 3B_0 f(1+2f)^{5/2}[1 + a_1 f + a_2 f^2 + \cdots], \tag{4}$$

with $a_1 = 3/2(B_0' - 4)$ and $a_2 = 3[B_0 B_0'' + B_0'(B_0' - 7) + (143/9)]/2$.

A relatively simple EOS was proposed by Huang and Chow (HC) [7]:

$$V/V_0 = 1 - a[1 - (1 + bP)^{-c}], \tag{5}$$

with $a = (1 + B_0')/(1 + B_0' + B_0 B_0'')$, $b = (B_0'/B_0) - [B_0''/(B_0' + 1)]$ and $c = (1 + B_0' + B_0 B_0'')/({B_0'}^2 + B_0' - B_0 B_0'')$.

Freund and Ingalls (FI) [10] modified the 'usual' Tait equation [12] as

$$V/V_0 = [1 - a\ln(1 + bP)]^c, \tag{6}$$

with the parameters $a = [\sqrt{({B_0'}^2 - 4B_0 B_0'')} - B_0']/[\sqrt{({B_0'}^2 - 4B_0 B_0'')} + B_0']$, $b = [\sqrt{({B_0'}^2 - 4B_0 B_0'')} + B_0']/2B_0$ and $c = 2[\sqrt{({B_0'}^2 - 4B_0 B_0'')} - B_0']$.

Recently we have proposed an EOS (SP) in the inverted form [12]:

$$V/V_0 = 1 - \{(\ln(1 + aP))/(b + cP)\}. \tag{7}$$

Here $a = (1/8B_0)[3(B_0' + 1) + (25{B_0'}^2 + 18B_0' - 32B_0 B_0'' - 7)^{1/2}]$, $b = (1/8)[3(B_0' + 1) + (25{B_0'}^2 + 18B_0' - 32B_0 B_0'' - 7)^{1/2}]$, and $c = [(1/16)[3(B_0' + 1) + (25{B_0'}^2 + 18B_0' - 32B_0 B_0'' - 7)^{1/2}]][(B_0' + 1) - (1/8)[3(B_0' + 1) + (25{B_0'}^2 + 18B_0' - 32B_0 B_0'' - 7)^{1/2}]]$.

The two-parameter EOS, proposed by Rose *et al* [31] and strongly promoted by Vinet *et al* as the so-called universal EOS [9], is founded on the well-known Rydberg empirical potential function. It will be interesting to study the applicability of the three-parameter extension of this model, which yields the following EOS (U3):

$$P = 3B_0(1 - x)(x^{-2})(\exp M). \tag{8}$$

Here, $M = (3/2)(B_0' - 1)(1 - x) + (3/2)(1 - x)^2[(1/4){B_0'}^2 + (1/2)B_0' + B_0 B_0'' - (19/36)]$, and $x = (V/V_0)^{1/3}$.

The bulk modulus, defined as $B = -V\,\mathrm{d}P/\mathrm{d}V$, can be expressed for an EOS of the form $V/V_0 = f(P)$, as

$$B = -f(P)/f'(P). \tag{9}$$

Three-parameter EOSs like B3, M3 and U3 are based upon Taylor series truncation. Higher-order bulk moduli terms are usually shorn off to restrict them to the two-parameter EOSs. The reason advanced is the paucity of information available for the requisite pressure derivatives of bulk modulus like B_0'', B_0''' and so on, and the assumption that the contributions from these higher-order bulk moduli terms are small compared to the lower-order terms. The contributions from the higher-order terms are. however, significant at large compressions [26, 51].

It might seem therefore that in fitting procedures, where adequate information on the bulk moduli terms is not a prerequisite, the inclusion of the higher-order bulk moduli terms might be justified in the study of experimental isotherms ranging up to large compressions. Further, it might be expected that an increasingly improved fit will be obtained with the inclusion of successively higher-order terms. But this is belied in practice. A plausible explanation for this paradoxical situation might be traced in the phenomenon, called polynomial wiggle [32]. The EOS data do not necessarily exhibit a 'polynomial nature' and the polynomials, underlying the EOSs, usually comprise increasingly complicated terms. Consequently the resulting curve to the data may exhibit large oscillations. This phenomenon, called polynomial wiggle, is,

in general, tangible as the number of parameters exceeds three and becomes increasingly pronounced with the inclusion of the higher-order terms beyond B_0''. Although the resulting curves may increasingly approach the data points or may even pass through these points, the fits become progressively worse. This conveys the simple message that the fitting accuracy alone, even if it is extraordinary, cannot certify the validity of an EOS. We have therefore restricted the comparison of our model to only the three-parameter extension of such EOSs.

3. Application to model-independent experimental isotherms

A good number of EOSs are now available in the literature, claiming varying degrees of success in the description of compressional behaviour of materials at high pressure. Therefore, it will be of practical interest to study the applicability of these EOSs. One of the most important tests, to discriminate between various EOSs, is the fitting accuracy between the data and fit, with no constraint on the parameters. Although a poor fit discredits an EOS, a good fit does not necessarily justify its acceptability, as discussed above. However, a high fitting accuracy between the data and fit obtained from a least-squares fit to the data is an important criterion when considered in conjunction with two other goodness-of-fit tests: agreement of the fitted bulk moduli parameters with those from the independent P–V measurements neat $P \sim 0$, and the stability of the fitted bulk moduli parameters with variation in the pressure/compression range [22]. An important condition, for a meaningful discrimination between EOSs, is obviously the model independence of the data to be fitted.

For the purpose of comparison, therefore, we have chosen model-independent isotherms of nine solids, differing considerably in their bulk modulus values, namely, Ag, Al, Mg, Pd, MgO [33], NaCl [34], Cu [35], Mo and W [36]. Nellis and co-workers [35] have proposed model-independent isotherms of Cu, Al and Pb, with pressures ranging up to the terrapascal regime. We have considered the isotherm of Cu only, because Cu is predicted to remain stable in the fcc structure up to at least 2.5 TPa [35] and thus projects the prospect of a possible pressure-calibration scale up to the ultrahigh pressure regime. It has also been shown that Cu is an excellent pressure marker in XAFS experiments with errors of not more than 0.5 GPa [37]. On the other hand, both Al and Pb are predicted and/or observed to exhibit structural phase transitions below 1 TPa [35, 38–40]. As such, the ultrahigh pressure isotherms of these elements are quite unlikely to be as accurate as that of Cu.

All the eight EOSs presented in section 2 are fitted to all the nine isotherms referred to above, and the resulting RMSD values in terms of V/V_0 or P are summarized in table 1. It may be noted that, for the sake of parity in comparison with the results of fitting, we have to use similar forms of the EOSs with respect to the dependent and independent variables. The B3 and U3 forms are explicitly expressed in the non-inverted form, $P = f(V/V_0)$, and cannot be changed to the inverted form, $V/V_0 = f(P)$. While the SP model, presented in the inverted form, cannot be explicitly expressed in the non-inverted form. The inverted form offers some advantages. It is useful in the analysis of EXAFS data of solids under high pressure [10]. Further, relative experimental errors in pressures are usually considerably smaller than those in volume. Therefore it is usually much preferable to fit experimental data to the inverted forms [22]. Results of curve-fitting corresponding to the inverted forms have been compared for all the EOSs except for B3 and U3. We have implicitly calculated the regression curves of P on V/V_0 for our equation SP and compared the results with those from the explicit curve fittings of P on V/V_0 for B3 and U3, for the sake of definitiveness in comparison. Throughout the following study, the values against the EOSs marked with an asterisk correspond to those resulting from the regression curves of P on V/V_0.

Table 1. Root-mean-square deviations (RMSDs) between data and fits. The RMSD values against the EOSs marked with an asterisk correspond to the regression curves of P on V/V_0 (in kbar). The rest of the values correspond to those of V/V_0 on P multiplied by 10^4.

	RMSD in $V/V_0(\times 10^4)$ or in P (in kbar)								
EOS	Ag [33]	Al [33]	Cu [35]	Mg [33]	Mo [36]	Pd [33]	W [36]	MgO [33]	NaCl [34]
SP	0.57	1.05	6.84	1.35	0.90	0.43	0.32	0.77	1.03
FI	2.04	2.05	14.35	2.91	1.46	1.34	0.89	0.85	1.06
HC	2.11	2.18	14.06	3.10	1.54	1.40	0.96	0.87	1.09
LU	2.44	2.74	13.19	3.67	1.82	1.68	1.25	0.96	1.07
KD	2.45	2.80	13.23	3.70	1.85	1.70	1.28	0.97	1.14
M3	2.48	2.93	13.30	3.78	1.92	1.73	1.36	0.98	1.35
SP*	0.28	0.21	17.80	0.19	1.03	0.24	0.41	0.24	0.08
B3*	0.81	0.43	25.56	0.27	1.25	0.72	0.66	0.26	0.085
U3*	0.91	0.49	31.20	0.40	1.35	0.82	0.74	0.30	0.095

3.1. Fitting accuracy

The following broad features on fitting accuracy can be readily discerned from table 1:

(i) All the EOSs fit the data very well.
(ii) Fitting accuracy, inferred from the SP expression, is higher than those from all seven EOSs for all the nine isotherms. Notably, except for the isotherms of NaCl and MgO where maximum compression does not exceed 30%, the fitting accuracy resulting from the SP expression is substantially higher for the rest of the isotherms, as implied by the RMSD values which are lower than those for the other EOSs by a factor of 2–4.
(iii) For all nine isotherms, the fitting accuracy of the B3 model is higher than its successor U3.
(iv) That LU equation fits all nine model-independent isotherms better than its successor, the KD.
(v) That, in general, the fitting accuracy of the EOSs decreases in the order SP > FI > HC > LU > KD > M3, and SP > B3 > U3 resulting from the regression curves of V/V_0 on P, and P on V/V_0, respectively.

Kumari and Dass [11] have claimed that their model fits Decker's room-temperature semitheoretical isotherms of NaCl and CsCl [41] better than the FI and HC models. The observation (v) prompted us to rework their calculated values. Contrary to their claim, our calculations show that the fitting accuracies obtained from the FI and HC EOSs are substantially higher than the KD model. The results of fitting the FI and HC EOSs to the isotherm of NaCl are: $B_0 = 238.3$ kbar, $B_0' = 4.739$, $B_0'' = -1.476\text{e}{-2}\,\text{kbar}^{-1}$ and RMSD $(V/V_0) = 0.68\text{e}{-4}$; and $B_0 = 238.5$ kbar, $B_0' = 4.715$, $B_0'' = -1.340\text{e}{-2}\,\text{kbar}^{-1}$ and RMSD $(V/V_0) = 0.77\text{e}{-4}$, respectively. While the results of fits for CsCl from the FI and HC EOSs are: $B_0 = 169.5$ kbar, $B_0' = 5.318$, $B_0'' = -2.468\text{e}{-2}\,\text{kbar}^{-1}$ and RMSD $(V/V_0) = 1.38\text{e}{-4}$; and $B_0 = 169.8$ kbar, $B_0' = 5.280$, $B_0'' = -2.217\text{e} - 2\,\text{kbar}^{-1}$ and RMSD $(V/V_0) = 1.60\text{e} - 4$, respectively.

Thus the fitting accuracies are in line with the relative performances observed here for the model-independent isotherms. Based on the values of the fit parameters calculated by Kumari and Dass [11], we had calculated the deviations between data and fits, plotted them in figures 1 and 2 of [12], and observed well-pronounced systematic biases with the FI and HC EOSs for both NaCl and CsCl. Contrary to these observations, we have now checked, on the basis of the reworked fit values from the FI and HC models (given above), that the deviations of the

data points are randomized well about the fit for both NaCl and CsCl (the deviation plots are not shown). The erroneous conclusion that crept up inadvertently in [12], for banking on the fit values published in [11], is regretted.

3.2. Fit parameters: stability and agreement with experiment

The important test of stability is based on the fact that, if an EOS applies well to a given set of data, it should apply as well to any partition of that set, and should yield (in the absence of experimental errors) the same parameter values [22]. To this end, each of the nine isotherms considered has been divided into three subsets, from the pressure values $P = 0$ to decreasing compression ranges. The EOSs 1–8 have a rather complicated functional form. Therefore, a minimum of eight measured data points is included in the lowest-pressure isotherm (LPI) to ensure that the statistical spirit of least-squares fitting is preserved. The fit parameter values of B_0, B_0' and B_0'' for all the subsets, along with the original isotherms, i.e. the highest-pressure isotherms (HPIs) resulting from all eight EOSs, are reported in table 2. Experimental values of B_0 and B_0' are presented in table 2 to facilitate an easy appreciation of their agreement with the fitted values of bulk moduli.

As can be seen in table 2, the fit values of B_0s, for the HPIs, are generally in good agreement with the experimental values, and no significant differences are noted between the EOSs, except in the case of the Nellis *et al* isotherm of Cu (N–Cu) [35]. In the case of N–Cu, the SP fit value of B_0 virtually coincides with the experimental value, while those from the rest of the EOSs deviate from experiment by about 17% to as large as 57%.

The percentage deviations of the fit values of B_0' (HPI), yielded by the different EOSs, from the experimental values are computed and compared in table 3. It is obvious from table 3 that, for the SP fit, the agreement with the experimental data is considerably better than that obtained with the other EOS models.

For NaCl, Fritz *et al* [34] have reported two sets of isotherms in their tables IV and VI, based on two types of fits to the primary shock-velocity (U_s)–particle velocity (U_p) data. In table IV, the maximum pressure extends to 250 kbar, while in table VI, a preferred isotherm with pressure ranging from 200 to 300 kbar is presented. To be on the assured side of accuracy, we have chosen the compression points of table IV up to 200 kbar only. Consequently, in the case of NaCl [34], the change in relative volume as we move from HPI to LPI is small, and also small are the values of the maximum pressure and compression range for the HPI. Thus no significant differences between the fit values of B_0 as well as B_0' and experiment are noted among the various EOSs.

Further, we have calculated the percentage deviations of the fit values of B_0, B_0' and B_0'' for the HPIs from those for the LPIs, corresponding to the four isotherms (three subsets and the HPI) for each solid (table 2) and summarized the results in tables 4–6. A glance at tables 4–6 clearly shows the drastic superiority of our model in terms of the stability of B_0, B_0' and B_0'' with variation in the pressure/compression ranges. The percentage deviation in B_0 calculated for the SP model is smaller than those for the other EOSs by a factor of 2 to as large as 6, while even larger differences are registered in the case of B_0's, especially for N–Cu. Even the variation of the fit values of B_0'', the uncertainty in the measured values of which is equal to or greater than its assigned values, obtained from the SP equation is decisively smaller than those from all seven EOSs compared, and for all nine model-independent isotherms considered.

The compression points of the N–Cu isotherm are wide apart from the stress-free state, i.e. the $(0, 0)$ data point, and they are also wide apart from each other. Only ten points are dispersed over the very large pressure range 0.1–1 TPa. Moreover, the data points are not uniformly distributed; eight points are within the pressure range of about 0.5 TPa and only

Table 2. Curve-fitting parameters B_0, B_0' and B_0'' as a function of pressure/compression range for selected solids. Here, A, B and C denote B_0 (kbar), B_0' and $B_0'' \times 10^{-4}$ (kbar^{-1}), respectively.

1. Ag (293 K) [33]: (Exp.: $B_0 = 1047$ kbar (average of [42] and [43]); $B_0' = 5.53$ [44])

	$Y_1 = 1500$; $Z_1 = 0.6519$			$Y_2 = 1000$; $Z_2 = 0.7011$			$Y_3 = 400$; $Z_3 = 0.8087$			$Y_4 = 145$; $Z_4 = 0.9017$		
Eq.	A	B	C	A	B	C	A	B	C	A	B	C
SP	1060	5.31	47.77	1060	5.32	48.35	1057	5.40	54.30	1055	5.46	60.07
FI	1071	4.99	14.34	1064	5.15	25.73	1057	5.38	49.07	1055	5.47	63.18
HC	1072	4.97	12.08	1065	5.13	23.15	1057	5.37	46.93	1055	5.47	63.23
LU	1075	4.89	4.854	1068	5.03	10.89	1059	5.30	31.03	1056	5.44	53.76
KD	1075	4.89	4.784	1068	5.03	10.69	1059	5.30	30.36	1056	5.43	50.17
M3	1075	4.89	4.645	1068	5.02	9.792	1059	5.28	26.84	1056	5.43	48.81
SP*	1061	5.29	47.59	1062	5.29	48.04	1058	5.38	53.63	1056	5.44	60.11
B3*	1080	4.92	19.43	1065	5.19	40.95	1057	5.43	68.31	1055	5.48	73.00
U3*	1083	4.81	1.526	1067	5.13	30.75	1057	5.42	65.43	1055	5.48	72.57

2. Al (293 K) [33]: (Exp.: $B_0 = 742 \pm 8$ kbar [45]; $B_0' = 4.72$ [46])

	$Y_1 = 1100$; $Z_1 = 0.6083$			$Y_2 = 550$; $Z_2 = 0.7085$			$Y_3 = 250$; $Z_3 = 0.8117$			$Y_4 = 100$; $Z_4 = 0.9010$		
	A	B	C	A	B	C	A	B	C	A	B	C
SP	767.6	4.29	57.36	765.2	4.35	61.44	762.4	4.46	76.21	758	4.79	171.7
FI	773.0	4.09	30.74	766.4	4.29	50.31	762.3	4.47	79.04	757.5	4.89	209.9
HC	773.4	4.07	27.07	766.6	4.28	47.90	762.1	4.48	81.29	757.2	4.93	237.6
LU	776.7	3.96	12.97	768.8	4.18	27.96	763.1	4.41	57.37	757.7	4.86	189.4
KD	777.1	3.95	12.16	769.0	4.17	26.27	763.2	4.40	54.02	757.8	4.84	174.9
M3	777.9	3.93	10.70	769.5	4.15	23.28	763.7	4.37	46.95	758.2	4.79	147.8
SP*	768.7	4.27	57.49	766.3	4.32	60.30	763.0	4.44	73.52	759.0	4.75	150.9
B3*	774.6	4.14	49.98	766.3	4.33	67.32	762.1	4.50	94.11	758.1	4.85	205.3
U3*	775.6	4.09	40.30	765.9	4.35	71.43	761.7	4.53	104.6	757.7	4.89	227.0

3. Cu (300 K) [35]: (Exp.: $B_0 = 1420$ kbar [42]; $B_0' = 5.25$ [47])

	$Y_1 = 10040$; $Z_1 = 0.436$			$Y_2 = 7280$; $Z_2 = 0.469$			$Y3 = 5420$; $Z3 = 0.502$		
	A	B	C	A	B	C	A	B	C
SP	1417	5.05	39.07	1427	5.01	38.33	1403	5.11	40.25
FI	1676	3.58	−37.61	1606	3.88	1.103	1507	4.36	11.21
HC	1673	3.61	−25.68	1612	3.85	0.468	1518	4.28	8.037
LU	1663	3.68	−7.915	1623	3.81	−1.340e−2	1556	4.06	1.959
KD	1663	3.68	−8.080	1623	3.81	−1.339e−2	1558	4.05	1.831
M3	1662	3.68	−8.388	1623	3.81	−1.339e−2	1563	4.03	1.617
SP*	1399	5.01	40.32	1472	4.86	35.88	1458	4.91	36.78
B3*	1871	3.17	2.511	1770	3.47	5.166	1602	4.12	16.73
U3*	2231	1.08	−62.13	1977	2.07	−48.93	1667	3.57	−12.36

4. Mg (293 K) [33]: (Exp.: $B_0 = 344.20$ kbar [48]; $B_0' = 4.16$ [48])

	$Y_1 = 700$; $Z_1 = 0.5510$			$Y_2 = 250$; $Z_2 = 0.7008$			$Y_3 = 115$; $Z_3 = 0.8052$			$Y_4 = 40$; $Z_4 = 0.9081$		
	A	B	C	A	B	C	A	B	C	A	B	C
SP	340.4	4.11	120.6	341.1	4.08	116.4	341.0	4.08	114.1	338.6	4.40	276.3
FI	348.3	3.76	35.34	342.2	3.97	74.85	341.2	4.04	92.69	338.6	4.43	298.6
HC	346.8	3.73	27.75	342.4	3.95	66.70	341.3	4.03	87.38	338.6	4.43	305.8
LU	348.2	3.66	12.47	343.0	3.89	40.88	341.6	3.99	62.24	338.6	4.41	261.6

Table 2. (Continued.)

KD	348.5	3.65	11.60	343.2	3.88	38.61	341.6	3.99	61.18	338.7	4.40	251.9
M3	348.7	3.64	10.56	342.8	3.89	37.52	341.7	3.98	56.53	338.6	4.40	233.9
SP*	339.1	4.14	125.6	341.7	4.05	115.7	341.8	4.02	105.2	338.6	4.42	270.8
B3*	347.0	3.83	81.54	342.3	4.01	109.5	341.6	4.03	108.7	337.9	4.56	397.2
U3*	351.6	3.57	3.747	342.4	3.99	97.45	341.7	4.02	101.2	337.9	4.58	436.6

5. Mo (293 K) [36] (Exp. $B_0 = 2653$ kbar [42]; $B_0' = 4.5 \pm 0.5$ [49])

	$Y_1 = 3000$; $Z_1 = 0.6305$			$Y_2 = 2000$; $Z_2 = 0.6919$			$Y_3 = 1300$; $Z_3 = 0.7540$			$Y_4 = 800$; $Z_4 = 0.8167$		
	A	B	C	A	B	C	A	B	C	A	B	C
SP	2673	3.89	14.36	2670	3.91	14.76	2668	3.92	14.97	2666	3.94	15.78
FI	2695	3.69	7.026	2679	3.80	9.8555	2672	3.86	11.76	2668	3.91	14.06
HC	2699	3.66	5.898	2679	3.79	9.084	2672	3.85	10.99	2667	3.91	13.63
LU	2709	3.58	3.123	2687	3.71	5.374	2677	3.79	7.315	2670	3.87	10.26
KD	2708	3.58	3.037	2688	3.70	5.037	2678	3.78	6.886	2670	3.86	9.515
M3	2712	3.56	2.673	2689	3.69	4.607	2678	3.77	6.252	2671	3.85	8.836
SP*	2674	3.88	14.60	2672	3.89	14.78	2668	3.91	15.08	2667	3.93	15.88
B3*	2697	3.75	12.03	2678	3.85	14.22	2670	3.90	15.52	2666	3.94	17.13
U3*	2704	3.68	8.523	2677	3.85	13.92	2669	3.91	16.07	2665	3.96	18.69

6. Pd (293 K) [33] (Exp.: $B_0 = 1808$ kbar [43]; $B_0' = 5.3 \pm 0.2$ [49])

	$Y_1 = 2000$; $Z_1 = 0.6831$			$Y_2 = 1150$; $Z_2 = 0.7501$			$Y_3 = 700$; $Z_3 = 0.8070$			$Y_4 = 250$; $Z_4 = 0.9018$		
	A	B	C	A	B	C	A	B	C	A	B	C
SP	1835	5.27	26.91	1834	5.29	27.69	1831	5.34	30.23	1830	5.35	28.35
FI	1847	5.03	10.42	1837	5.19	18.28	1832	5.31	26.53	1831	5.33	27.07
HC	1847	5.02	9.320	1837	5.18	17.03	1832	5.31	26.23	1831	5.33	26.92
LU	1852	4.94	4.234	1841	5.10	9.558	1834	5.24	16.71	1831	5.32	22.50
KD	1852	4.94	4.161	1840	5.10	9.215	1834	5.23	15.70	1831	5.31	20.52
M3	1852	4.93	3.852	1841	5.09	8.614	1826	5.37	21.10	1831	5.31	20.13
SP*	1837	5.25	27.02	1835	5.27	27.57	1832	5.33	30.33	1831	5.33	28.23
B3*	1856	5.01	15.57	1836	5.25	28.26	1830	5.38	38.28	1830	5.35	31.28
U3*	1861	4.92	6.986	1837	5.22	24.53	1830	5.37	36.62	1831	5.34	31.32

7. W (293 K) [36]: (Exp.: $B_0 = 3084$ kbar [50]; $B_0' = 4.0 \pm 0.2$ [49])

	$Y_1 = 3000$; $Z_1 = 0.6552$			$Y_2 = 2000$; $Z_2 = 0.7154$			$Y_3 = 1300$; $Z_3 = 0.7754$			$Y_4 = 800$; $Z_4 = 0.8347$		
	A	B	C	A	B	C	A	B	C	A	B	C
SP	3107	3.95	12.68	3105	3.96	12.87	3102	3.98	13.35	3098	4.02	14.83
FI	3127	3.78	7.037	3111	3.88	9.369	3104	3.94	11.22	3099	4.01	14.34
HC	3129	3.76	6.204	3114	3.86	8.559	3104	3.94	11.01	3099	4.01	14.27
LU	3140	3.68	3.439	3120	3.79	5.275	3109	3.88	7.477	3101	3.97	10.75
KD	3141	3.67	3.228	3122	3.78	4.994	3110	3.87	7.044	3101	3.96	9.993
M3	3143	3.66	2.945	3122	3.77	4.531	3112	3.85	6.252	3102	3.95	9.282
SP*	3110	3.93	12.75	3106	3.95	13.04	3104	3.96	13.22	3097	4.03	15.37
B3*	3127	3.84	11.25	3109	3.93	13.11	3105	3.96	13.98	3096	4.05	17.45
U3*	3131	3.80	9.387	3109	3.93	13.11	3103	3.98	14.94	3095	4.07	19.22

Table 2. (Continued.)

	8. MgO (293 K) [33]: (Exp.: $B_0 = 1560$ kbar [52]; $B_0' = 4.52$ [53])											
	$Y_1 = 1200$; $Z_1 = 0.7046$			$Y_2 = 850$; $Z_2 = 0.7500$			$Y_3 = 550$; $Z_3 = 0.8036$			$Y_4 = 200$; $Z_4 = 0.9017$		
	A	B	C	A	B	C	A	B	C	A	B	C
SP	1530	4.50	26.60	1531	4.48	25.70	1531	4.47	24.79	1528	4.57	40.25
FI	1536	4.34	12.57	1534	4.38	15.09	1533	4.40	16.56	1528	4.59	43.26
HC	1536	4.33	11.33	1534	4.37	13.72	1533	4.40	16.08	1528	4.60	46.02
LU	1538	4.28	6.519	1535	4.33	8.713	1533	4.37	10.90	1528	4.57	35.46
KD	1538	4.28	6.399	1536	4.32	8.273	1534	4.36	10.47	1528	4.56	32.71
M3	1538	4.27	5.877	1535	4.32	7.784	1534	4.36	10.20	1529	4.55	33.08
SP*	1529	4.50	27.41	1530	4.48	26.57	1532	4.45	25.08	1531	4.47	27.03
B3*	1534	4.41	22.67	1532	4.44	24.32	1532	4.43	23.14	1530	4.52	36.21
U3*	1536	4.35	15.42	1533	4.40	18.79	1533	4.41	19.69	1530	4.53	38.84
	9. NaCl (293 K) [34]: (Exp.: $B_0 = 238.35$ kbar [20]; $B_0' = 5.11$ [18])											
	$Y_1 = 200$; $Z_1 = 0.7023$			$Y_2 = 120$; $Z_2 = 0.7706$			$Y_3 = 75$; $Z_3 = 0.8252$			$Y_4 = 40$; $Z_4 = 0.8849$		
	A	B	C	A	B	C	A	B	C	A	B	C
SP	238.7	5.23	292.4	238.5	5.25	298.2	238.2	5.28	309.6	239.3	5.15	280.2
FI	237.8	5.35	359.7	238.2	5.31	344.0	238.2	5.31	344.9	239.3	5.16	293.2
HC	237.5	5.39	390.0	238.1	5.33	362.3	238.2	5.31	350.3	239.3	5.16	294.6
LU	239.8	5.08	184.5	239.0	5.15	205.5	238.5	5.22	236.3	239.4	5.12	225.5
KD	240.2	5.03	162.1	239.2	5.12	186.9	238.6	5.20	219.3	239.4	5.12	221.5
M3	241.2	4.93	126.3	239.7	5.06	156.1	238.8	5.17	194.6	239.4	5.11	204.2
SP*	238.6	5.24	291.8	238.9	5.22	287.9	237.8	5.34	335.9	239.4	5.14	274.1
B3*	235.9	5.59	558.4	237.5	5.45	492.1	237.1	5.50	523.1	239.0	5.23	385.1
U3*	234.6	5.74	650.9	237.2	5.50	532.6	237.0	5.52	545.4	239.0	5.23	387.8

Table 3. Agreement of the fit parameter B_0' for the HPI with experiment for selected solids. The values in parentheses, in the column under Mo, represent the deviations from the lower limit of the experimental value of $B_0' = 4.0$ for Mo. Experimental values of B_0' are given in table 2.

	% deviation in the fit value of B_0' (HPI) from experiment							
EOS	Ag [33]	Al [33]	Cu [35]	Mg [33]	Mo [36]	Pd [33]	W [36]	MgO [33]
SP	4.0	9.1	3.8	1.2	13.6(2.8)	0.6	1.3	0.4
FI	9.8	13.3	31.9	9.6	18.0(7.8)	5.1	5.5	4.0
HC	10.1	13.8	31.2	10.3	18.7(8.5)	5.3	6.0	4.2
LU	11.6	16.1	29.9	12.0	20.4(10.5)	6.8	8.0	5.3
KD	11.6	16.3	29.9	12.3	20.4(10.5)	6.8	8.3	5.3
M3	11.6	16.7	29.9	12.5	20.9(11.0)	7.0	8.5	5.5
SP*	4.3	9.5	2.9	0.5	13.8(3.0)	0.9	1.8	0.4
B3*	11.0	12.3	39.6	7.9	16.7(6.3)	5.5	4.0	2.4
U3*	13.0	13.3	79.4	14.2	18.2(8.0)	7.2	5.0	3.8

two points are above it. Further, an abrupt increase in the pressure ranges results in an abrupt decrease in the rate of decrease of V/V_0. Thus the error variance of the data points of N–Cu is not homogeneous due to the non-uniform data variability. A high degree of flexibility on the part of the EOSs is called for, to describe such data curves accurately. For N–Cu, the

Table 4. Percentage deviation in the fit values of B_0 for the HPI from those of B_0 for the LPI.

	% deviation in the fit value of B_0 (HPI) from B_0 (LPI)] $\times[-1]$								
EOS	Ag [33]	Al [33]	Cu [35]	Mg [33]	Mo [36]	Pd [33]	W [36]	MgO [33]	NaCl [34]
SP	0.47	1.27	1.71	0.74	0.26	0.27	0.29	0.20	0.46
FI	1.52	2.05	11.21	2.27	1.01	0.87	0.90	0.52	0.63
HC	1.61	2.14	10.21	2.42	1.20	0.87	1.00	0.52	0.76
LU	1.80	2.51	6.88	2.83	1.46	1.15	1.26	0.65	0.55
KD	1.80	2.55	6.74	2.89	1.42	1.15	1.29	0.65	0.67
M3	1.80	2.60	6.33	2.98	1.54	1.42	1.32	0.59	1.01
SP*	0.47	1.28	5.22	0.95	0.26	0.33	0.42	0.20	0.67
B3*	2.37	2.18	16.79	2.69	1.16	1.42	1.00	0.26	1.31
U3*	2.65	2.36	33.83	4.05	1.46	1.69	1.16	0.39	1.88

Table 5. Percentage deviation in the fit values of B_0' for the HPI from those of B_0' for the LPI.

	% deviation in the fit value of B_0' (HPI) from B_0' (LPI)								
EOS	Ag [33]	Al [33]	Cu [35]	Mg [33]	Mo [36]	Pd [33]	W [36]	MgO [33]	NaCl [34]
SP	2.8	10.4	1.2	6.6	1.3	1.5	1.7	1.5	−1.6
FI	8.8	16.4	17.9	15.1	5.6	5.6	5.7	5.5	−3.7
HC	9.1	17.4	15.7	15.8	6.4	5.8	6.2	5.9	−4.5
LU	10.1	18.5	9.4	17.0	7.5	7.1	7.3	6.4	0.8
KD	9.9	18.4	9.1	17.1	7.3	7.0	7.3	6.1	1.8
M3	9.9	18.0	8.7	17.3	7.5	7.2	7.3	6.2	3.5
SP*	2.8	10.1	−3.9	6.3	1.3	1.5	2.5	−0.7	−2.0
B3*	10.2	14.6	23.1	16.0	4.8	6.4	5.2	2.4	−6.9
U3*	12.2	16.4	69.8	22.1	7.1	7.9	6.6	4.0	−9.8

Table 6. Percentage deviation in the fit values of B_0'' for the HPI from those of B_0'' for the LPI.

	% deviation in the fit value of B_0'' (HPI) from B_0'' (LPI)								
EOS	Ag [33]	Al [33]	Cu [35]	Mg [33]	Mo [36]	Pd [33]	W [36]	MgO [33]	NaCl [34]
SP	20.5	66.6	2.9	56.4	9.0	5.1	14.5	33.9	−4.4
FI	77.3	85.4	435.5	88.2	50.3	61.5	50.9	70.9	−22.7
HC	80.9	88.6	419.5	90.9	56.7	65.4	56.5	75.4	−32.4
LU	91.0	93.2	504.0	95.2	69.6	81.2	68.0	81.6	18.2
KD	90.5	93.1	541.3	95.4	68.1	79.7	67.7	80.4	26.8
M3	90.5	92.8	618.7	95.5	69.7	80.9	68.3	82.2	38.2
SP*	20.8	61.9	−9.6	53.6	8.1	4.3	17.1	−1.4	−6.5
B3*	73.4	75.7	85.0	79.5	29.8	50.2	35.5	37.4	−45.0
U3*	97.9	82.3	−402.7	99.1	54.4	77.7	51.2	60.3	−67.8

performance of the SP equation on all three counts: the fitting accuracy, agreement of the fit values of B_0 and B_0' (for HPIs) with experiment, and stability of these fit values with variation in the pressure/compression ranges, is remarkably good; and extraordinarily better than all seven EOSs compared. This reflects the robust behaviour of the SP model. The B3 model does not behave well, and the behaviour of U3 is the worst of all. It will be interesting to note

that the poor performance of the B3 equation for the accurate representation of data has also been noted earlier by Anderson *et al* [8] and by Greene *et al* [45] for isotherms ranging to low-and high-pressure regimes, respectively.

As can be seen (from table 2) the fit parameter values for the regression curves of V/V_0 on P and the regression curves of P on V/V_0, for the isotherms of all the nine solids yielded by the SP EOS, are nearly equal. The differences between the two sets of values are the estimates of the errors incurred by data fit, and are significantly small. The obvious conclusion is that our model describes the EOS data very well.

Focusing on the LPIs, a spectacular convergence of the EOSs can be noted, except for the isotherm of N–Cu. The fitted values of B_0 are equal or very nearly equal. Although the fitted values of B_0' are not as close to each other as in the case of B_0, still their mutual agreement is quite appreciable. The maximum disagreement between the fit value of B_0' is registered in the case of MgO, and it is only about 4%. Even the fit values of the highly unreliable B_0'' do not differ significantly. The RMSD values are also virtually indistinguishable (the results are not shown). These observations accord well with the assertions of MacDonald and Powell [30] that the bulk moduli parameters derived from fitting $V(P)$ data at low pressures ($P < 0.1B_0$) are independent of the analytical form of the EOSs used, and thus discrimination between EOSs is not possible in the low-pressure regime.

Further, it may be noted that the fit bulk moduli values for the LPI, especially those of B_0 and B_0', may be considered as the closest approximation to their real values. This explains why we have assessed the stability of the fit bulk moduli parameters, with variation in the compression ranges, in terms of their deviations from the fit values generated for the LPIs. In fact, all the fit values of B_0 for the LPI of the different materials agree with the experimental values within about 2%, except for Ag. For Ag, the measured value of $B_0 = 1087$ kbar [42] is higher than the value of 1007 kbar obtained from [43] by about 8%. While the LPI fit values of B_0 for Ag, from the different EOSs, differ from these measured values by about 3–5%, respectively. Thus, the wide mutual deviations between the measured values, as well as their comparatively larger deviations from the LPI fit values, indicate that both these measured values are probably not accurate. Therefore we have presented the average of these two values in table 2. Of the limited measured bulk modulus values we have access to, those closest to the LPI fit values have been presented in table 2, and hence the selection of these measured bulk modulus values for the comparative purposes is not arbitrary.

The LPI fit values of B_0' for all the isotherms and from all the EOSs (in the case of N–Cu, only from the SP EOS) agree with the experimental values within about 10%, except for Mo. Both the LPI and HPI fit values of B_0' for Mo deviate considerably from experiment (table 2), exceeding above 10%. As such, the experimental value of B_0' (4.5 ± 0.5) for Mo is probably not accurate. However, on considering the value corresponding to the lower limit of uncertainty, the experimental value of B_0' for Mo comes down from 4.5 to 4.0, and it matches well the LPI fit values of B_0' from all the EOSs considered. A plausible justification for considering the lower limit value of B_0' is that the LPI fit values from all the EOSs are clearly lower than 4.0. The deviations of the HPI fit values of B_0' from the lower limit of the experimental value of 4.0 are given in parentheses in table 3, and obviously the SP model is remarkably closer to the data than the rest of the EOSs.

In the case of Al, the LPI fit values are generally in very good agreement with experiment, but the agreement becomes progressively worse as we move up the pressure regime. To illustrate the point, the SP fit value of B_0' for LPI ($P_{\max} = 100$ kbar) deviates from experiment only by about 1.5%, which increases to as large as about a 9% deviation from experiment when we reach HPI ($P_{\max} = 1100$ kbar). Further, it may be noted that the fit value of B_0' (HPI, $P_{\max} = 1100$ kbar) deviates from that of B_0' (LPI, $P_{\max} = 100$ kbar) by about 10%, whereas

a deviation as large as 7%, in the fit value of B_0', is registered when we move from LPI to an isotherm with a P_{max} of only 250 kbar (table 2). Although Geene *et al* have not detected any structural phase transitions in Al up to a pressure of 2200 kbar [45], contrary to the earlier observations [35], it is highly probable that Al undergoes phase changes in the relatively small pressure region 100–250 kbar, as indicated above. This probability needs to be investigated with the help of improved techniques.

Further, it may be noted that the temperature of measurement of the bulk moduli differs by a few degrees from the temperature of the isotherms (table 2). But the error incurred in the comparative study between the fit parameters and experiment is inappreciable. It will be interesting to note that the fit values of B_0 (LPI) for NaCl at 293 K, on correcting to 300 K in line with Birch [6], are about 238.2 kbar from the SP, FI and HC, and 238.3 kbar from the LU, KD, M3 and SP* fitting exercises, in excellent agreement with the measured value of 238.4 kbar of Spetzler *et al* [20]. The LPI fit values of B_0', for which the effect of correction for temperature is small, are in good agreement with the value of 5.11 from Kim [18], except for the B3 and U3 EOSs, which yield B_0' values that lie intermediate between those of Kim and Spetzler *et al*.

4. Variation of bulk modulus with pressure

For the purpose of our study we haven chosen the ultrasonic data on ionic solid NaCl at 300 K [20] and the piston-displacement data on the inert gas solid neon at 4.2 K [23]. Employing the fitted values of bulk moduli parameters for the Fritz *et al* isotherm of NaCl at 293 K (from table 2) and the Anderson *et al* isotherm for Ne at 4.2 K (from table 8), and using equation (9), we have calculated the values of bulk modulus at different pressures up to 10 kbar for NaCl and up to 20 kbar for Ne, respectively. For NaCl, the bulk modulus data points have been corrected to 293 K in line with Birch [6]. Percentage deviations of the calculated values of bulk modulus from the data points have been estimated for both NaCl and Ne and the results are shown in figure 1. For both solids, the deviations rise to a maximum value of about 0.5% only, and thus a very good agreement is noted.

5. Compatibility with first principles approaches

In order to test an EOS model, it is not necessary to test it against theoretical values, because the ultimate test of any methodology is its agreement with experiment. Some of the EOSs in the literature have a partial theoretical support. But all of them are, in essence, empirical because none of them is derived from fundamental structural energetics. The theoretical basis of a completely empirical EOS is not immediately apparent, either due to our incapability as such to decipher them or the present-day theoretical knowledge is not adequate to explain and/or to account for the intricacies of experiment, the Nature. It is not surprising therefore that attempts still continue to give a new physical interpretation of the pressure coefficient parameter of the century-old Tait equation [54]. In fact, many-body forces, appropriate for a condensed phase, are effectively absorbed in an empirical EOS. It will be interesting, however, to see to what extent our empirical model is compatible with the first principles approaches.

CsI

Aidun and co-workers [24] carried out augmented-plane-wave (APW) calculations to generate a room-temperature (298 K) compression curve for CsI up to a pressure of about 75 GPa. Huang and Ruoff [55] have reported an experimental EOS for CsI and reported that CsI transforms to a

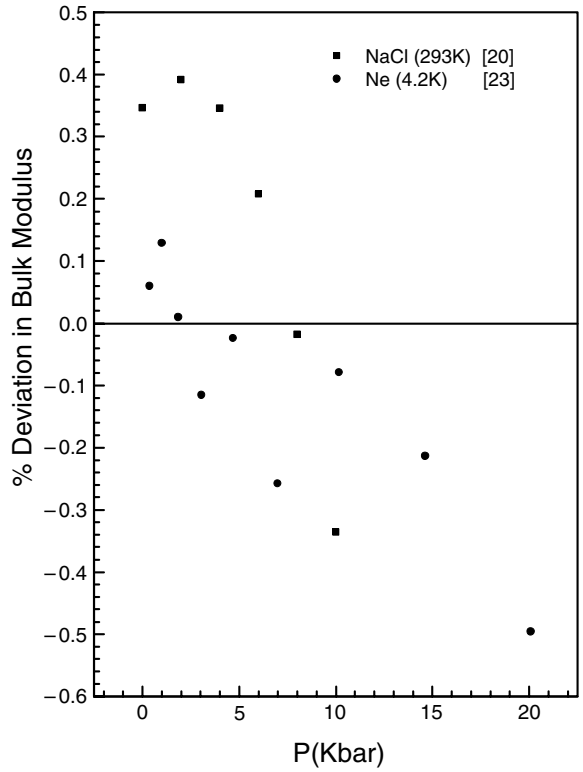

Figure 1. Percentage deviations of the values of bulk modulus predicted by the SP equation, from experiment, for the solids NaCl (293 K) [20] and Ne (4.2 K) [23].

new crystallographic structure at 40 GPa. We have therefore fitted our model to the theoretical isotherm up to a pressure of 35.69 GPa only. The fit parameters are $B_0 = 12.28$ GPa, $B_0' = 5.514$ and $B_0'' = -0.5095$ GPa^{-1}, with an RMSD value of 2.63×10^{-4}. The fit values of B_0 and B_0' are higher than the experimental data [56] by about 2 and 7%, respectively. The agreement is good in view of the fact that the uncertainties in their theoretical isotherms arise from the approximations inherent in the APW method, computational error and their use of Debye theory and quasiharmonic lattice dynamics, which neglect the temperature dependence of γ and provide a volume dependence that is untested by experiment.

MgO

A knowledge of the thermodynamic properties of MgO at simultaneous high pressures and temperatures is important in the study of the Earth's lower mantle, but experimental constraints disallow their measurements. Isaak *et al* [25], using the PIB model, and resorting to a number of approximations and assumptions, including those which help to increase computational efficiency and provide a larger slant towards experiment, calculated the P–V–T relations of MgO along with the values of the bulk modulus and its pressure derivatives over a wide P–T space [26].

The results of fitting equations SP, B3 and U3 to the five theoretical isotherms of MgO are shown in table 7. It will be interesting to note that, although our model does not have apparent theoretical support, unlike the B3 and U3 models, it matches the theoretical isotherms better

Table 7. Fit parameter B_0'' (multiplied by -10^2) along with RMSDs for the regression curves of P on V/V_0 for the theoretical isotherm of MgO [26] at different temperatures from the SP, B3 and U3 equations. B_0 and B_0' are constrained to the theoretical values.

EOS	T (K)	B_0 (GPa)	B_0'	$B_0'' \times (-10^2)$ (GPa^{-1})	RMSD in P (GPa)
	300	180 (fixed)	4.15 (fixed)		
SP*				2.4	0.90
B3*				2.6	0.63
U3*				2.6	0.30
	500	175 (fixed)	4.21 (fixed)		
SP*				2.6	0.28
B3*				2.8	0.49
U3*				2.9	0.37
	1000	160 (fixed)	4.36 (fixed)		
SP*				3.0	0.18
B3*				3.3	0.28
U3*				3.5	0.27
	1500	144 (fixed)	4.53 (fixed)		
SP*				3.5	0.28
B3*				4.0	0.42
U3*				4.2	0.31
	2000	128 (fixed)	4.74 (fixed)		
SP*				4.3	0.72
B3*				5.2	0.30
U3*				5.5	0.34

than them at three temperatures: 500, 1000 and 1500 K. Using the fit values of the bulk moduli for the SP EOS at five temperatures, pressures are calculated as a function of V/V_0, and also bulk modulus as a function of pressure. Deviations of the calculated pressures and bulk modulus values from the theoretical points are plotted in figures 2 and 3, respectively. It can be seen in figure 2 that about 75% of the predicted pressure points agree with the theoretical values within about 0.5% and 15% within a range of about 0.5–1%, while the rest 10% of the predicted points agree within a range of about 1–1.8% only. Figure 3 shows that only two predicted bulk modulus points disagree by well over 2%, one at 300 K (about 5%) and the other at 2000 K (about 3%), while five predicted points deviate up to about 2%, with the rest agreeing to within about 1% only. Thus the overall agreement is good.

6. Application to a wide variety of solids

In this section we will show that equation (7) can be applied to study the compression data of a wide variety of materials. It may be emphasized, however, that our model is not universal, and no universal EOS is known to date. A universal EOS is applicable to all types of solids, irrespective of their bonding characteristics, provided that the solids possess the desired homogeneity to behave as an elastic continuum. It has been identified by seismology that the Earth's lower mantle and outer core are regions that are homogeneous in composition and mineral structure over wide pressure ranges [57]. Since our model is not compatible with the bulk moduli measurements of these homogeneously close-packed materials, it is denied a universal status.

The compression data of most of the solids are taken from the *AIP Handbook* [58], except those of Rb [8], Li and Cs [59], Ne [23], Ar, Kr and Xe [60] and NaCl [61]. The calculated

Table 8. Curve-fitting parameters along with RMSDs (in V/V_0) from the SP expression for the isotherms of selected solids. RMSD and B_0'' are multiplied by 10^4 and -10^3, respectively. The isotherms are taken from the *AIP Handbook* [58], except those of Rb [8], Li, Cs [59], Ne [23], Ar, Kr, Xe [60] and NaCl [61].

Sl no	Solid inorganic	P_{max} (kbar)	$(V/V_0)_{min}$	B_0 (kbar)	B_0'	$B_0'' \times (-10^3)$ (kbar^{-1})	RMSD $\times(10^4)$
1	Be	800	0.698	1196	3.61	3.349	2.4
2	Ca	360	0.465	192.7	2.7	6.02	3.2
3	Cd	1000	0.613	502.1	5.63	11.87	2.6
4	Co	1200	0.730	1961	4.33	2.455	2.6
5	Ni	1200	0.735	1884	4.71	2.539	2.8
6	Pt	2000	0.728	2808	5.07	1.860	2.8
7	Sn	600	0.649	435.7	5.30	12.63	2.8
8	Ta	1800	0.655	1978	3.77	2.063	2.7
9	Th	1000	0.552	522.4	4.11	8.542	2.7
10	Ti	2000	0.512	979.8	3.63	4.148	3.1
11	Tl	340	0.770	355.5	5.45	16.01	2.7
12	V	1000	0.713	1583	3.74	2.263	2.9
13	Zn	2500	0.521	597.2	5.69	10.39	5.0
14	Zr	1400	0.527	942.7	2.89	3.342	2.7
15	Al_2O_3	1200	0.757	2515	3.90	1.540	2.8
16	CsBr	550	0.505	217.8	4.09	20.88	3.5
17	CsCl	220	0.651	177.8	4.98	30.28	4.3
18	KI	180	0.571	93.79	4.52	52.21	3.4
19	LiBr	240	0.653	220.3	4.47	21.40	2.7
20	LiF	800	0.640	626.4	4.77	8.143	2.7
21	LiCl	220	0.712	328.5	3.95	10.65	2.6
22	LiI	280	0.616	328.6	2.54	8.280	3.0
23	NaBr	240	0.638	209.1	4.27	21.75	3.0
24	NaCl	236.8	0.6803	238.8	5.21	287.3	1.7
25	NaI	240	0.613	198.5	3.88	21.34	2.6
26	RbBr	160	0.575	76.60	4.86	67.98	4.1
27	RbCl	120	0.602	58.68	5.44	98.59	3.6
28	RbF	240	0.605	150.4	4.68	33.34	2.6
29	RbI	180	0.572	94.49	4.53	52.21	2.6
30	Li (294 K)	19.52	0.875	115.5	3.54	26.51	0.20
31	Cs (295 K)	19.39	0.625	16.63	4.19	304.8	1.60
32	Rb (295 K)	48.30	0.550	22.83	4.39	194.7	1.07
33	Ar (4 K)	20	0.770	28.72	7.33	292.6	0.28
34	Ar (20 K)	20	0.767	27.77	7.345	297.0	0.18
35	Ar (40 K)	20	0.754	23.58	7.555	353.8	0.31
36	Ne (4.2 K)	20	0.677	11.06	7.547	738.3	0.10
37	Ne (13.5 K)	20	0.672	10.36	7.605	791.8	0.14
38	Ne (19.9 K)	20	0.659	8.357	8.084	1068	0.20
39	Kr (4 K)	20	0.785	33.47	7.349	254.6	0.27
40	Kr (20 K)	20	0.783	31.6	7.492	259.7	0.06
41	Kr (40 K)	20	0.772	27.91	7.629	297.6	0.16
42	Xe (20 K)	20	0.792	35.65	7.376	238.2	0.20
43	Xe (40 K)	20	0.786	33.12	7.490	256.9	0.24
44	Xe (60 K)	20	0.779	30.32	7.527	278.4	0.25
	Alloy						
45	Brass	850	0.717	1174	4.69	4.143	3.0

Table 8. (Continued.)

Sl no	Solid inorganic	P_{max} (kbar)	$(V/V_0)_{min}$	B_0 (kbar)	B_0'	$B_0'' \times (-10^3)$ (kbar^{-1})	RMSD $\times(10^4)$
	Glass						
46	Glass A	100	0.825	294.1	5.673	13.47	3.13
47	Glass C	100	0.841	395.0	3.639	−25.11	5.36
48	Glass D	100	0.833	244.6	9.978	100.2	6.03
49	Pyrex glass	100	0.807	96.93	4.27	−169.6	4.8
50	Quartz glass	100	0.797	99.97	3.74	−128.0	6.3
	Organic						
51	Acenaphthylene	40	0.808	70.34	8.37	86.34	3.7
52	Anthracene	40	0.808	60.00	11.51	347.3	5.0
53	Benzil	40	0.787	31.74	11.80	33.62	8.2
54	Bezophenone	24	0.835	62.77	8.61	239.4	3.9
55	Cyanamide	40	0.838	121.4	7.80	151.1	4.1
56	Diphenyl	40	0.784	46.30	10.57	331.3	7.9
57	Hexamethylenetetramine	40	0.827	84.70	10.56	273.3	5.7
58	Iodoform	40	0.794	74.89	6.64	57.4	4.4
59	*M*-acetyltoluidine	40	0.783	64.87	6.47	39.23	4.6
60	Menthol	24	0.806	49.85	9.70	591.6	5.6
61	Methylcyclohexane	40	0.646	9.09	10.00	1209	8.8
62	*M*-iodobenzoic acid	40	0.812	80.17	7.26	25.19	7.5
63	Morpholine hydrogen tartrate	40	0.845	122.9	8.25	137.8	4.3
64	*M*-toluidine hydrochloride	40	0.792	60.75	8.15	115.9	3.3
65	*O*-aminobenzene sulfonic acid	40	0.841	113.4	5.89	−121.8	3.7
66	*O*-aminophenol	40	0.827	81.25	9.49	114.8	7.4
67	*O*-chlorobenzoic acid	40	0.814	78.05	8.29	100.8	3.8
68	*O*-dicresyl carbonate	40	0.793	66.73	6.47	−25.67	8.9
69	*O*-methylnitrocinnamate	40	0.804	66.62	9.77	249.8	4.0
70	*P*-aminobenzoic acid	40	0.817	94.26	5.03	−135.5	7.8
71	*P*-diphenylbenzene	40	0.805	59.40	10.23	222	7.6
72	*P*-nitroaniline	40	0.821	78.53	10.00	215.3	3.5
73	*P*-nitroiodobenzene	40	0.814	71.07	9.74	195.2	3.8
74	*P*-nitrophenol	40	0.813	85.51	6.35	−25.73	4.3
75	*P*-phenylenediamine hydrochloride	40	0.821	88.79	6.55	−56.54	4.0
76	*P*-toluic acid	40	0.790	63.84	7.85	121.1	3.4
77	Thymol	30	0.806	52.77	7.77	69.27	4.5
78	Triphenylmethane	40	0.796	70.98	6.64	17.57	7.8
79	Urea nitrate	40	0.842	123.1	6.34	−18.85	2.0
	Plastic						
80	Laminac 4201	40	0.793	50.93	11.04	348.9	5.50
81	Cellulose acetate	40	0.767	45.96	8.24	174.1	4.5
82	Lucite	40	0.780	49.93	8.88	193.6	6.4
83	Nylon 6-10	40	0.785	55.56	7.53	55.88	5.2
84	Silicone 160	40	0.759	12.13	16.81	1584	6.9
85	Fluorine plastic	40	0.803	50.09	10.32	177.7	5.19
	Rubber						
86	Hevea gum	24	0.790	25.90	11.63	622.3	5.8
87	Koroseal 89023	24	0.796	26.52	11.17	449.5	6.6
88	Neoprene 832	24	0.802	27.76	14.30	1014	6.0

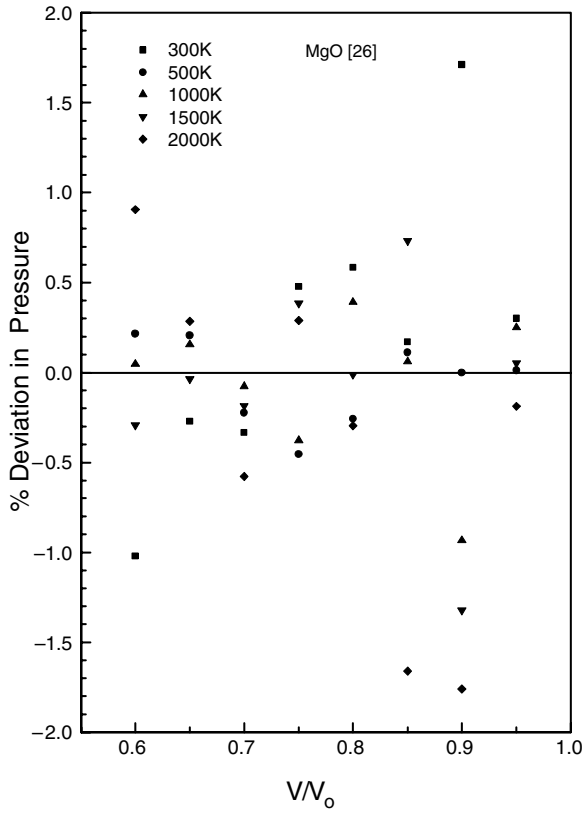

Figure 2. Percentage deviations of the SP-predicted pressures from the theoretical pressure points for MgO [26] at different temperatures.

values of the fitted bulk moduli parameters B_0, B_0' and B_0'', along with the resulting RMSD values in terms of V/V_0, are summarized in table 8 for inorganic and organic solids including alloys, glasses, plastics and rubbers. We have access to some experimental values on bulk modulus for inorganic solids (not shown). It is observed that the overall agreement between the data and fit is good.

We have no access to any experimental values for the bulk modulus of the organic solids in table 8. In the case of the isotherms of the organic solids studied, both the pressure and compression ranges are small. We have noted, however, that the fitted bulk modulus values, even of B_0s for the organic solids from the various EOSs, differ from each other by a wide margin, unlike those for the inorganic solids. Thus it appears that, in the future, the availability of accurate and model-independent isotherms of organic solids and their reliable experimental bulk moduli values might prove useful for a more tangible discrimination between the various EOSs of solids, even in the low-pressure and low-compression region.

7. Summary

Three important tests have been performed to discriminate between eight EOSs, in respect of applicability to the EOS data, using model-independent isotherms of nine solids of divergent bulk modulus values, and with pressures ranging from low to a maximum that varies from the

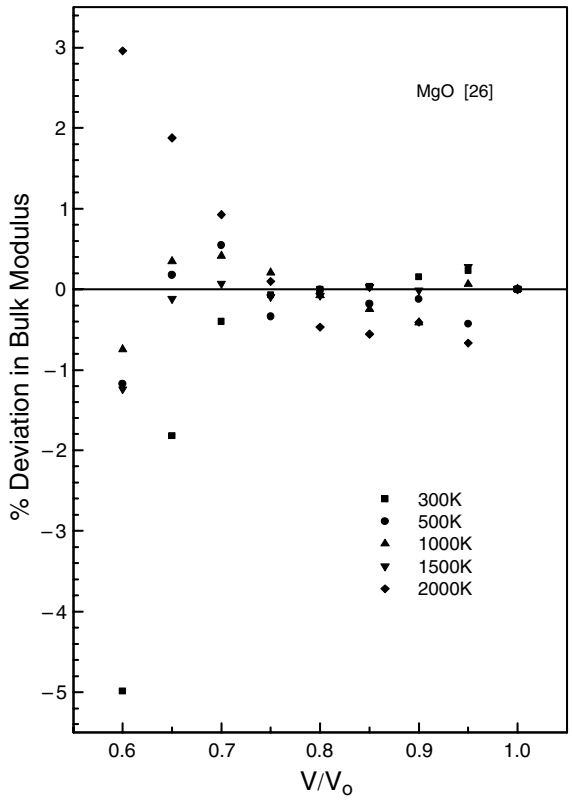

Figure 3. Percentage deviations of the SP-predicted bulk modulus values from the theoretical calculations for MgO [26] at different temperatures.

high to ultrahigh pressure regime. The calculated results decisively demonstrate the drastic superiority of our proposed model on an overall assay. It is observed that the model proposed by Luban [8] is, in general, better than its successor, the KD model [11]. Likewise, the B3 model is decisively better than its successor, the U3 model. For the Nellis *et al* isotherm of Cu, with pressure ranging up to the terrapascal regime, the performance of all the EOSs, as contrasted with the excellent performance of our model, is poor—the fit values of both B_0 and B_0' deviate considerably from the experimental values. The performance of the much acclaimed B3 model is quite discouraging, while that of the U3 model is the worst of all. An inter-comparison of the results obtained for the nine solids indicates that the fitting accuracy, stability of the fit parameters with variation in the compression range, and agreement of the fit parameters with experiment are interrelated; and some systematics is exhibited in that, in general, they decrease in the order SP > FI > HC > LU > KD > M3 and SP > B3 > U3. Further, our model fits well the compression data of solids of widely divergent bonding characteristics, as demonstrated by the high fitting accuracy obtained for a large variety of solids. Finally, the present study indicates that the value of B_0' for Mo probably lies in the close vicinity of 4.0.

Acknowledgment

We are grateful to Professor Bertil Sundqvist, Department of Experimental Physics, Umea University, Sweden for helping us find some references.

References

[1] Tait P G 1888 *Phys. Chem.* **2** 1
[2] Dymond J H and Malhotra R 1988 *Int. J. Thermophys.* **9** 941
[3] Murnaghan F D 1944 *Proc. Natl Acad. Sci. USA* **30** 244
[4] Murnaghan F D 1967 *Finite Deformation of an Elastic Solid* (New York: Dover)
[5] Birch F 1952 *J. Geophys. Res.* **57** 227
[6] Birch F 1978 *J. Geophys. Res.* **83** 1257
[7] Huang Y K and Chow C Y 1974 *J. Phys. D: Appl. Phys.* **7** 2021
[8] Anderson M S and Swenson C A 1983 *Phys. Rev.* B **28** 5395
[9] Vinet P, Ferrante J, Smith J R and Rose J H 1986 *J. Phys. C: Solid State Phys.* **19** L467
[10] Freund J and Ingalls R 1989 *J. Phys. Chem. Solids* **51** 263
[11] Kumari M and Dass N 1990 *J. Phys.: Condens. Matter* **2** 3219
[12] Bose Roy S and Bose Roy P 1999 *J. Phys.: Condens. Matter* **11** 10375
[13] Hofmeister A M 1991 *J. Geophys. Res.* **96** 21893
[14] Birch F 1986 *J. Geophys. Res.* **91** 4949
[15] Ruoff A L and Chhabildas L C 1978 *High Pressure Science and Technology, 6th AIRAPT Conf.* vol 1, ed K D Timmerhans and M S Barber (New York: Plenum) pp 19–32
[16] Hofmeister A M 1997 *Phys. Rev.* B **56** 5835
[17] Sorensen Y S 1983 *J. Geophys. Res.* **88** 3543
[18] Kim H S, Graham E K and Voigt D E 1989 *Trans. Am. Geophys. Union* **70** 1368
[19] Truell R, Elbaum C and Chick B B 1969 *Ultrasonic Methods in Solid State Physics* (CA: Academic) p 464
[20] Spetzler H, Sammis C G and O'Connell R J 1972 *J. Phys. Chem. Solids* **33** 1727
[21] Chhabildas L C and Ruoff A L 1976 *J. Appl. Phys.* **47** 4182
[22] Macdonald J R 1966 *Rev. Mod. Phys.* **38** 669
[23] Anderson M S, Fugate R Q and Swenson C A 1973 *J. Low Temp. Phys.* **10** 314
[24] Aidun J, Bukowinski M S T and Ross M 1984 *Phys. Rev.* B **29** 2611
[25] Isaak D G 1990 *J. Geophys. Res.* **95** 7055
[26] Anderson O L 1995 *Equations of State of Solids for Geophysical and Ceramic Science* (New York: Oxford University Press)
[27] Jeanloz R 1988 *Phys. Rev.* B **38** 805
[28] Sikka S K 1988 *Phys. Rev.* B **38** 8463
[29] Holzapfel W B 1996 *Rep. Prog. Phys.* **59** 29
[30] Macdonald J R and Powell D R 1971 *J. Res. NBS* A **75** 441
[31] Rose J H, Smith J R, Guinea F and Ferrante J 1984 *Phys. Rev.* B **29** 2963
[32] Mathews J H 1994 *Numerical Methods for Mathematics, Science and Engineering* 2nd edn (New Delhi: Prentice-Hall) p 278
[33] Carter W J, Marsh S P, Fritz J N and McQueen R G 1971 *Accurate Characterization of the High Pressure Environment Special Publication* NBS Circular no 326 ed E C Lyod (Washington, DC: US Government Printing Office) p 147
[34] Fritz J N, Marsh S P, Carter W J and McQueen R G 1971 *Accurate Characterization of the High Pressure Environment Special Publication* NBS Circular no 326 ed E C Lyod (Washington, DC: US Government Printing Office) p 201
[35] Nellis W J, Moriarty J A, Mitchell A C, Ross M, Dandrea R G, Aschcroft N W, Holmes N C and Gathers G R 1988 *Phys. Rev. Lett.* **60** 1414
[36] Hixson R S and Fritz J N 1992 *J. Appl. Phys.* **71** 1721
[37] Freund J and Ingalls R 1989 *Phys. Rev.* B **39** 12537
[38] Moriarty J A and McMahan A K 1982 *Phys. Rev. Lett.* **48** 809
[39] McMahan A K and Moriarty J A 1983 *Phys. Rev.* B **27** 3235
[40] Takahashi T, Mao H K and Basset W A 1969 *Science* **165** 1352
[41] Decker D L 1971 *J. Appl. Phys.* **42** 3239
[42] Simmons G and Wang H 1971 *Single Crystal Elastic Constants and Calculated Aggregate Properties* 2nd edn (Cambridge, MA: MIT Press)
[43] Kittel C 1976 *Introduction to Solid State Physics* 5th edn (New York: Wiley)
[44] Ullmann W and Pan'kov V L 1976 Zentralinstitut fur Physik der Erde, Potsdam
[45] Greene R G, Luo H and Ruoff A L 1994 *Phys. Rev. Lett.* **73** 2075
[46] Swenson C A 1968 *J. Phys. Chem. Solids* **29** 1337
[47] Vant't Klooster P, Traphenters N J and Biswas S N 1979 *Physica* B **97** 65

[48] Anderson O L 1966 *J. Phys. Chem. Solids* **27** 547
[49] Holzapfel W B 1997 *High-Pressure Techniques in Chemistry and Physics* ed W B Holzapfel and N S Isaacs (New York: Oxford University Press) p 47
[50] Wang K and Reeber R R 1997 *High Temp. Mater. Sci.* **36** 185
[51] Jeanloz R 1992 *High Pressure Research in Geophysics* ed M H Manghnani and S Akimoto (Tokyo: Centre of Academic Publications) p 147
[52] Mao H K and Bell P M 1979 *J. Geophys. Res.* **84** 4533
[53] Anderson O L and Andreatch P Jr 1966 *J. Am. Ceram. Soc.* **49** 404
[54] Baonza V G, Caceres M and Nunez Z 1995 *Phys. Rev.* B **51** 28
[55] Huang T L and Ruoff A L 1984 *Phys. Rev.* B **29** 1112
[56] Barch G R and Chang Z P 1971 *Accurate Characterization of the High Pressure Environment Special Publication* NBS Circular no 326 ed E C Lyod (Washington, DC: US Government Printing Office) p 173
[57] Stacey F D 1999 *J. Phys.: Condens. Matter* **11** 575
[58] Kennedy G C and Keeler R N 1972 *American Institute of Physics Handbook* 3rd edn, ed D E Gray (New York: McGraw-Hill)
[59] Anderson M S and Swenson C A 1985 *Phys. Rev.* B **31** 668
[60] Anderson M S and Swenson C A 1975 *J. Phys. Chem. Solids* **36** 145
[61] Brown J M 1999 *J. Appl. Phys.* **86** 5801